Pergamon

*Int. J. Solids Structures* Vol. 32, No. 10, pp. 1405–1416, 1995

0020–7683/95 $9.50 + .00

0020–7683(94)00191–X

# NONLINEAR ANALYSIS OF LAMINATED NON-CIRCULAR CYLINDRICAL SHELLS

MARINA FIRER and IZHAK SHEINMAN
Faculty of Civil Engineering, Technion–Israel Institute of Technology, Technion City 32000, Israel

(*Received* 31 *January* 1994; *in revised form* 28 *July* 1994)

**Abstract**—The nonlinear analysis of laminated initially imperfect non-circular cylindrical shells is presented. The analytical model is based on Donnell's nonlinear kinematic relations. The equations are derived via the Hu–Washizu mixed formulation, and are expressed in terms of the transverse displacement and the Airy stress function. The curvature of the non-circular cross-section is expanded into a Fourier series, allowing for representation of arbitrary closed cross-sections. The solution procedure is based on expansion of the variables into truncated trigonometric series in the circumferential direction and a finite difference scheme in the longitudinal one. Errors introduced by the truncated series are minimized by the Galerkin procedure and the equations are linearized by the Newton–Raphson method. Solutions beyond the limit point are obtained by Riks' constant arc-length algorithm. Results of both isotropic and laminated, axially loaded oval and elliptic shells are presented. The non-circular configurations are found to be less imperfection sensitive than the circular ones, and for largely eccentric cross-sections the shells are insensitive to initial imperfections.

## INTRODUCTION

Cylindrical shell structures are commonly used in structural engineering. Their buckling and post-buckling behaviour is of vital importance in the design of such structures. Being highly imperfection sensitive, nonlinear analysis is essential in understanding the behaviour of cylindrical shells.

While the behaviour of circular cylindrical shells has been extensively studied (see Simitses, 1986), relatively few deal with the stability problem of non-circular cylindrical shells. The buckling problem of non-circular isotropic shells is studied by Kempner and Chen (1964, 1967), Hutchinson (1968), Feinstein *et al.* (1971a,b), Chen and Kempner (1976) and Volpe *et al.* (1978, 1980). The analysis of laminated non-circular shells is presented in Soldatos and Tzivanidis (1982), Sun (1991) and Sheinman and Firer (1994). In all cited work, only the linear bifurcation analysis and initial post-buckling solution of Donnell type equations are presented and the authors are not aware of results of the full nonlinear analysis of non-circular cylindrical shells. Except for Sheinman and Firer (1994), the analysis is confined to either elliptic or oval cross-sections.

In the present paper, the post-buckling problem of non-circular cylindrical shells is considered and a solution algorithm suitable for the nonlinear analysis of initially imperfect cylindrical shells of arbitrary closed cross-section is presented. Being a periodic function of the circumferential angle, the shape of the cross-section is described in terms of a Fourier series. The governing equations are derived from an energy principle, based on Donnell type kinematic relations, which are sufficiently accurate for the analysis of shells with buckling patterns involving several circumferential waves. The analysis is based on the classical laminate theory and equations are expressed in terms of the transverse displacement and the Airy stress function. Solution is based on expansion of the variables into truncated Fourier series in the circumferential direction and a finite difference scheme in the longitudinal one. The equations are linearized by the Newton–Raphson method and errors introduced by the truncated series are minimized by the Galerkin procedure. Equilibrium states beyond the limit points are computed by Riks' constant arc-length algorithm.

The proposed algorithm is initially validated in the analysis of a circular cylindrical shell. Solutions for both oval and elliptic isotropic cylindrical shells are presented. Finally, the effect of the fiber orientation in angle-ply laminated oval shells is investigated.

## MATHEMATICAL FORMULATION

Let $(x, y, z)$ be the coordinate system measured with respect to the reference surface in the axial, circumferential and radial direction, respectively. Let $u$, $v$ and $w$ be the components of the displacements (in the $x$, $y$ and $z$ direction, respectively) of any point in the mid-surface of the shell. Further, let $\Delta w(x, y)$ be the initial geometric imperfection of the shell. Application of the Kirchhoff–Love hypothesis as basic assumptions, and resorting to the von Karman nonlinear kinematic approach, the strain–displacement relations at any point of the shell can be written as

$$\{\varepsilon\} = \{\varepsilon_0\} + z\{\kappa\}, \tag{1}$$

where $\{\varepsilon_0\}$ and $\{\kappa\}$ are the strains and changes of curvature at the mid-surface given by

$$\{\varepsilon_0\} = \begin{Bmatrix} u_{,x} + \frac{1}{2}w_{,x}^2 + w_{,x}\Delta w_{,x} \\ v_{,y} - \dfrac{w}{R(y)} + \frac{1}{2}w_{,y}^2 + w_{,y}\Delta w_{,y} \\ u_{,y} + v_{,x} + w_{,x}w_{,y} + w_{,x}\Delta w_{,y} + w_{,y}\Delta w_{,x} \end{Bmatrix} \tag{2}$$

$$\{\kappa\} = \begin{Bmatrix} -w_{,xx} \\ -w_{,yy} \\ -2w_{,xy} \end{Bmatrix}.$$

$(\ )_{,x}$ and $(\ )_{,y}$ denote the derivatives in the axial ($x$) and circumferential ($y$) directions, respectively and the curvature $R$ is a function of the circumferential coordinate.

Under the classical laminate theory, the strain $\{\varepsilon_0\}$ and bending moment $\{M\} = \{M_{xx}, M_{yy}, M_{xy}\}^T$ can be expressed in terms of the internal membrane forces $\{N\} = \{N_{xx}, N_{yy}, N_{xy}\}^T$ and changes of curvature $\{\kappa\}$ as

$$\{\varepsilon_0\} = [a]\{N\} - [b]\{\kappa\}$$

$$\{M\} = [b]^T\{N\} + [d]\{\kappa\}$$

where $a = A^{-1}$, $b = A^{-1}B$ and $d = D - BA^{-1}B$. $A$, $B$ and $D$ are, respectively, the membrane, coupling and bending stiffnesses, defined as

$$(A_{ij}\, B_{ij}\, D_{ij}) = \int_z Q_{ij}(1\ z\ z^2)\,\mathrm{d}z \tag{3}$$

where $Q_{ij}$ are the plane stress reduced elastic stiffnesses of the laminate.

Introducing the Airy stress function ($F$) will enable reduction of the problem to two dependent variables ($w$ and $F$) only. The stress function is defined by the following relationship:

$$\{N\} = \{\mathbf{F}\} + \{\bar{N}\} \tag{4}$$

where $\{\mathbf{F}\} = \{F_{,yy}, F_{,xx}, -F_{,xy}\}^T$ is the Airy stress vector and $\{\bar{N}\} = \{\bar{N}_{xx}, \bar{N}_{yy}, \bar{N}_{xy}\}^T$ is the external in-plane loading applied at the boundaries.

The governing field and boundary equations in $w$ and $F$ are derived via the Hu–Washizu mixed formulation for the potential energy (see Sheinman and Firer, 1994)

$$\Pi = \int_x \int_y \left\langle \frac{1}{2}\left( -\{\mathbf{F}+\bar{N}\}^{\mathrm{T}}[a]\{\mathbf{F}+\bar{N}\} + 2\{\mathbf{F}+\bar{N}\}^{\mathrm{T}}[b]\{\kappa\} + \{\kappa\}^{\mathrm{T}}[d]\{\kappa\} \right.\right.$$
$$+ (F_{,yy}+\bar{N}_{xx})(w_{,x}^2 + 2\Delta w_{,x} w_{,x}) + (F_{,xx}+\bar{N}_{yy})(w_{,y}^2 + 2\Delta w_{,y} w_{,y})$$
$$\left.\left. -2(F_{,xy}+\bar{N}_{xy})(w_{,x}w_{,y} + \Delta w_{,x} w_{,y} + \Delta w_{,y} w_{,x}) - 2(F_{,xx}+\bar{N}_{yy})\frac{w}{R}\right) - qw \right\rangle \mathrm{d}x\,\mathrm{d}y \quad (5)$$

where $q$ is the external applied normal pressure. Variation of $\Pi$ yields the following equilibrium and compatibility nonlinear equations:

$$\mathscr{L}_{\bar{a}}(w) - \mathscr{L}_{\bar{b}}(F) + \mathscr{L}(F, w+\Delta w) - \mathscr{L}_1(w+\Delta w) - \frac{(F_{,xx}+\bar{N}_{yy})}{R} = q$$

$$\mathscr{L}_{\bar{b}}(w) + \mathscr{L}_{\bar{a}}(F) + \frac{1}{2}\mathscr{L}(w, w+2\Delta w) - \frac{(w_{,xx})}{R} = 0 \quad (6)$$

where the differential operators $\mathscr{L}_k$, $\mathscr{L}$ and $\mathscr{L}_1$ are defined as

$$\mathscr{L}_k(S) = k_{40}S_{,xxxx} + k_{31}S_{,xxxy} + k_{22}S_{,xxyy} + k_{13}S_{,xyyy} + k_{04}S_{,yyyy}$$
$$\mathscr{L}(S,T) = S_{,xx}T_{,yy} - 2S_{,xy}T_{,xy} + S_{,yy}T_{,xx}$$
$$\mathscr{L}_1(S) = \bar{N}_{xx}S_{,xx} + 2\bar{N}_{xy}S_{,xy} + \bar{N}_{yy}S_{,yy} \quad (7)$$

with $k = \bar{a}$, $\bar{b}$ and $\bar{d}$. The coefficients $\bar{a}_{ij}$, $\bar{b}_{ij}$ and $\bar{d}_{ij}$ are expressed in terms of the laminate properties $[a]$, $[b]$ and $[d]$ and are listed in Sheinman *et al.* (1988).

The boundary conditions are derived in the same manner as in Sheinman and Simitses (1977) and allow for simply supported $SS_i$, clamped $CC_i$ and free $FF_i$ edges. The subscript $i = 1,\ldots,4$ denotes the following in-plane conditions: $i = 1$ for $F_{,xy} = F_{,yy} = 0$; $i = 2$ for $F_{,xy} = 0$, $u = c$; $i = 3$ for $v = F_{,yy} = 0$; $i = 4$ for $v = 0$, $u = c$, where $c$ is a constant.

The average end-shortening of the shell is defined as

$$e_{\mathrm{av}} = \frac{1}{2\pi R_0 L}\int_x \int_y \langle a_{11}(F_{,yy}+\bar{N}_{xx}) + a_{12}(F_{,xx}+\bar{N}_{yy}) + a_{13}(-F_{,xy}+\bar{N}_{xy})$$
$$+ b_{11}w_{,xx} + b_{12}w_{,yy} + 2b_{13}w_{,xy} - \tfrac{1}{2}w_{,x}(w_{,x}+2\Delta w_{,x})\rangle \,\mathrm{d}x\,\mathrm{d}y. \quad (8)$$

In order to accomodate for arbitrary cross-sections (see Sheinman and Firer, 1994), the radius of curvature of the non-circular cross-section is described by a truncated Fourier series, in which the number of terms used will be set according to the desired geometry. The present study is confined to cross-sections with at least two axes of symmetry, thus

$$\frac{1}{R(\theta)} = \sum_{k=0}^{NR} \alpha_k \cos(2k\theta) \quad (9)$$

where $\theta$ is the angular coordinate and $NR$ is the number of terms in the truncated series for the curvature. The curvatures of oval and elliptic cross-sections, which are widely discussed in the literature (see for example Kempner and Chen, 1967; Hutchinson, 1968; Volpe *et al.*, 1980; Sun, 1991) can be exactly described, as shown in Sheinman and Firer (1994).

Since the Fourier expansion of the curvature is written in terms of the angular coordinate ($\theta$) rather than the circumferential one ($y$), the field and boundary equations must be written in terms of the angular coordinate. The transformation is effected through the differential operators $\mathscr{L}_k$, $\mathscr{L}$ and $\mathscr{L}_1$, defined in eqn (8) as

$$\begin{aligned}\bar{\mathscr{L}}_k(S) &= k_{40}S_{,xxxx}+k_{31}rS_{,xxx\theta}+k_{22}(rr_{,\theta}S_{,xx\theta}+r^2S_{,xx\theta\theta})\\ &+k_{13}(rr_{,\theta}^2S_{,x\theta}+r^2r_{,\theta\theta}S_{,x\theta}+3r^2r_{,\theta}S_{,x\theta\theta}+r^3S_{,x\theta\theta\theta})\\ &+k_{04}(rr_{,\theta}^3S_{,\theta}+4r^2r_{,\theta}r_{,\theta\theta}S_{,\theta}+r^3r_{,\theta\theta\theta}S_{,\theta}+7r^2r_{,\theta}^2S_{,\theta\theta}+4r^3r_{,\theta\theta}S_{,\theta\theta}+6r^3r_{,\theta}S_{,\theta\theta\theta}+4r^4S_{,\theta\theta\theta\theta})\end{aligned}$$

$$\bar{\mathscr{L}}(S,T) = S_{,xx}(rr_{,\theta}T_{,\theta}+r^2T_{,\theta\theta})-2r_{,\theta}^2S_{,x\theta}T_{,x\theta}+(rr_{,\theta}S_{,\theta}+r^2S_{,\theta\theta})T_{,xx} \tag{10}$$

$$\bar{\mathscr{L}}_1(S) = \bar{N}_{,xx}S_{,xx}+2\bar{N}_{,xy}rS_{,x\theta}+\bar{N}_{,yy}(rr_{,\theta}S_{,\theta}+r^2S_{,\theta\theta})$$

where $r = r(\theta) = 1/R(\theta)$.

## SOLUTION METHODOLOGY

In the same manner as in Sheinman and Firer (1994), the set of partial differential equations is reduced to one of the ordinary differential equations by separation of variables and expansion of the axial variables into truncated Fourier series as

$$w(x,\theta) = \sum_{m=0}^{2NW} w_m(x)g_m(\theta)$$

$$F(x,\theta) = \sum_{n=0}^{2NF} F_n(x)g_n(\theta), \tag{11}$$

$NW$ and $NF$ being the number of retained terms in the truncated series for $w$ and $F$, respectively, and

$$g_m(\theta) = \begin{cases}\cos(im\theta) & m = 0,1,\ldots,N\\ \sin(im\theta) & m = N+1,\ldots,2N.\end{cases} \tag{12}$$

$N = NW$ for the $w$-series and $N = NF$ for the $F$-series; $i$ denotes the characteristic circumferential wave number. Recourse to a characteristic wave number makes it possible, in some cases, to substantially reduce the number of terms in the Fourier series (Narasimham and Hoff, 1967). For general cases, in which all terms are significant, it is necessary to let $i = 1$ and $NW$ and $NF$ sufficiently large for an accurate representation of $w$ and $F$. The initial geometric imperfection is treated in the same manner as the transverse deflection $w$, i.e.

$$\Delta w(x,\theta) = \sum_{m=0}^{2NW} \Delta w_m(x)g_m(\theta) \tag{13}$$

allowing for representation of arbitrary initial imperfections, including those in the shape of the natural buckling modes of the perfect shell, which have a predominant effect on the behaviour of the shell (Arbocz, 1974).

Minimizing the errors due to the truncated Fourier series by applying the Galerkin procedure, with $\cos(im\theta)$ and $\sin(im\theta)$ as weighting functions, yields the following ordinary differential equations.

*Equilibrium equations.*

$$\sum_{m=0}^{2NW}\{\bar{d}_{40}A_0(m,p)w_{m,xxxx}+\bar{d}_{31}A_1(m,p)w_{m,xxx}+[\bar{d}_{22}A_2(m,p)-\bar{N}_{xx}A_0(m,p)]w_{m,xx}$$

$$+[\bar{d}_{13}A_3(m,p)-2\bar{N}_{xy}A_1(m,p)]w_{m,x}+[\bar{d}_{04}A_4(m,p)-\bar{N}_{yy}A_2(m,p)]w_m\}$$

$$+\sum_{n=0}^{2NF}\{\bar{b}_{40}A_0(n,p)f_{n,xxxx}+\bar{b}_{31}A_1(n,p)f_{n,xxx}$$

$$+[\bar{b}_{22}A_2(n,p)+B_1(n,p)]f_{n,xx}+\bar{b}_{13}A_3(n,p)f_{n,x}+\bar{b}_{04}A_4(n,p)f_n\}$$

$$+\sum_{m=0}^{2NW}\sum_{n=0}^{2NF}\{C_1(m,n,p)f_n(w_{m,xx}+\Delta w_{m,xx})$$

$$-2C_2(m,n,p)f_{n,x}(w_{m,x}+\Delta w_{m,x})+C_1(m,n,p)f_{n,xx}(w_m+\Delta w_m)\}$$

$$=\delta 2\pi q+\bar{N}_{yy}B_0(p)+\sum_{m=0}^{2NW}[\bar{N}_{xx}A_0(m,p)\Delta w_{m,xx}$$

$$+2\bar{N}_{xy}A_1(m,p)\Delta w_{m,x}+\bar{N}_{yy}A_2(m,p)\Delta w_m]$$

$$p=0,1,\ldots,2NW. \tag{14}$$

*Compatibility equations.*

$$\sum_{m=0}^{2NW}\{\bar{b}_{40}A_0(m,p)w_{m,xxxx}+\bar{b}_{31}A_1(m,p)w_{m,xxx}$$

$$+[\bar{b}_{22}A_2(m,p)+B_1(m,p)]w_{m,xx}+\bar{b}_{13}A_3(m,p)w_{m,x}+\bar{b}_{04}A_4(m,p)w_m\}$$

$$+\sum_{n=0}^{2NF}\{\bar{a}_{40}A_0(n,p)f_{n,xxxx}+\bar{a}_{31}A_1(n,p)f_{n,xxx}$$

$$+\bar{a}_{22}A_2(n,p)f_{n,xx}+\bar{a}_{13}A_3(n,p)f_{n,x}+\bar{a}_{04}A_4(n,p)f_n\}$$

$$+\sum_{m=0}^{2NW}\sum_{k=0}^{2NW}\{C_1(m,k,p)(w_m w_{k,xx}+w_m\Delta w_{k,xx}+w_{m,xx}\Delta w_k)$$

$$-2C_2(m,k,p)w_{m,x}(w_{k,x}+\Delta w_{k,x})\}=0$$

$$p=0,1,\ldots,2NF \tag{15}$$

where $\delta=1$ for $p=0$ and $\delta=0$ otherwise. The expressions for the Galerkin coefficients $A_i(m,p)$, $B_i(m,p)$ and $C_i(m,n,p)$ are given in Sheinman and Firer (1994). The boundary equations for all $SS_i$, $CC_i$ and $FF_i$ boundary conditions are treated in the same way, and are expressed as functions of the meridional coordinate only (see Firer, 1993).

By increasing the number of dependent variables from two ($w$ and $F$) to four ($w, \phi, F, \psi$) where

$$\phi_m = w_{m,xx}$$

$$\psi_n = F_{n,xx},$$

the set of fourth order equations is reduced to a set of second order nonlinear differential ones, and the number of equations is doubled. The nonlinear equations are solved by the Newton–Raphson method and by the aid of a central finite difference scheme in the meridional direction. Equilibrium states beyond limit points are computed by the constant arc-length algorithm (Riks, 1979).

## NUMERICAL RESULTS AND DISCUSSION

The above outlined procedure is implemented in a general computer code, able to handle both bifurcation buckling (see Sheinman and Firer, 1994) and full nonlinear analysis of laminated cylindrical shells of arbitrary cross-sections. The program is especially suitable for parametric studies of the effect of the ovality and laminate layup as well as of boundary conditions. The solution methodology for the nonlinear response (far beyond the limit point) is demonstrated through examples of isotropic and laminated non-circular cylindrical shells under axial compression.

*Isotropic cylindrical shell*

Results from the proposed algorithm and convergence of the solution for the different parameters are initially examined in a isotropic circular cylindrical shell with geometric data taken from Volpe *et al.* (1980): length to radius ratio $L/R = 0.7$, radius to thickness ratio $R/h = 100$, Poisson ratio $v = 0.3$ and $SS_3$ boundary conditions. An initial axisymmetric imperfection [$\Delta w = 0.1h \sin(\pi x/L)$] is assumed, and solution is required to converge to a 0.1% accuracy. Two finite difference meshes (25 and 35 nodes) were checked, yielding similar results. The 25 node mesh is thus adopted for all further analyses. Results are normalized by the classical buckling load $N_{cl} = Eh^2/[R\sqrt{3(1-v^2)}]$. As seen in Fig. 1, results are in very good agreement with those calculated by the procedure of Sheinman and Simitses (1983) with $NW = 1$ and $NF = 2$. It should be noted that, although the Fourier terms computed by the two algorithms are completely different, the total displacement at a given point is in very good agreement. These discrepancies and the differences in post-buckling stage are due to the different formulations on which the two algorithms are based. Figure 1 presents also the results based on a ten-term approximation of the variables ($NW = NF = 10$, characteristic wave number $i = 1$). While pre-buckling behaviour of the shell is not affected by the addition of Fourier terms, the post-buckling behaviour is clearly influenced, as a result of changes in the characteristic buckling wave (see also Sheinman and Simitses, 1983) which are not accounted for in the more limited analysis. The effect of the initial imperfection shape is shown in Fig. 2. Changes in characteristic waves in the post-buckling stage are clearly seen. The smallest post-buckling stiffness is obtained when the imperfection is assumed in the shape of the bifurcation buckling mode. Convergence of both the linear (bifurcation) and nonlinear analyses of oval shells [represented by $R_0/R(\theta) = 1 + \xi \cos(2\theta)$ where $\xi$ is the eccentricity parameter and $R_0$ is the radius of an equivalent circular cylinder having the same perimeter as the oval one] with the number of Fourier terms and influence of the characteristic wave number are summarized in Fig. 3. The imperfection in this example, as in all further ones, is taken as the bifurcation shape with maximum amplitude of $\Delta w_{max} = 0.1h$. Both bifurcation and limit points converge from above, while the minimum post-buckling load presents no defined convergence trend. Bifurcation and limit point loads computed by the ten-term expansions ($NW = NF = 10$, $i = 1$) are in very good agreement with the more exact ones ($NW = NF = 20$, $i = 1$) for all ranges of ovality. When the characteristic wave number is taken as $i = 2$, the influence of coupling between odd Fourier terms is not accounted for (see Sheinman and Firer, 1994). This results in higher bifurcation and limit point loads, mainly in the small eccentric ovals ($\xi \leqslant 0.3$). The discrepancies in the minimum point loads are explained by the changes in the post-buckling behaviour which is governed by coupling of a very large number of circumferential waves. The average end-shortening of various ovals are plotted in Fig. 4. It is clearly seen that, as the eccentricity of the oval cross-section increases, the shell is less imperfection sensitive, resulting in large post-buckling stiffnesses. For eccentricities larger than $\xi \approx 0.75$, the shell is insensitive to imperfections.

The use of an equivalent circular cylinder [$R_{eq} = R_0/(1-|\xi|)$ where $R_{eq}$ is the radius of curvature of the weakest region of the oval cross-section, where the buckling process initiates] proposed by Volpe *et al.* (1980) as an estimate for the behaviour of oval shells, is studied in Fig. 5. Both short length ($L/R_0 = 0.7$) and medium length ($L/R_0 = 2.0$) shells with $CC_1$ boundary conditions are studied. The equivalent radius estimate is conservative for almost all ranges of eccentricity, and yields good results for small eccentric configurations; for eccentricities larger than 0.4 it is too conservative, especially in longer

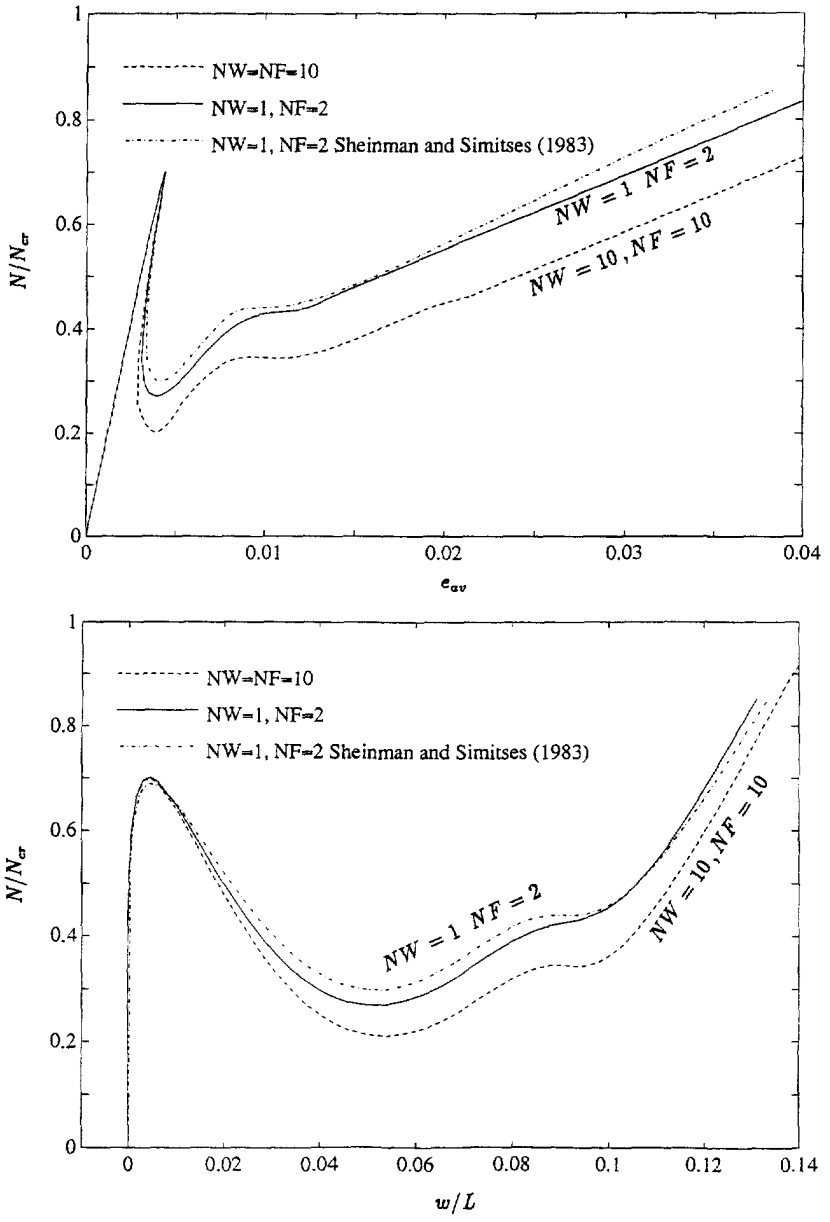


Fig. 1. Total midpoint deflection and average end-shortening of circular cylindrical shells.

shells. This is explained by the decrease of the sensitivity of the oval configuration to initial imperfections. Finally, the elliptic cross-section is considered through expansion of the curvature into a Fourier series [see Sheinman and Firer (1994) for the classical buckling behaviour]. The results for the post-buckling stage, versus those of oval cross-sections are listed in Table 1 and plotted in Fig. 6. For the nearly circular cross-sections, both the bifurcation and limit point loads of the two cross-sections are in good agreement. For the two other cases, discrepancies of around 40% between results for oval and elliptic cross-sections are observed. It seems that in the medium eccentricity case this can be attributed to the fact that the minimum curvature of the elliptic cross-section is significantly lower than the corresponding oval one, resulting in lower buckling loads for the elliptic cross-section. In the large eccentricity case, though minimum curvatures of the two cross-sections are almost the same, the elliptic cross-section shows a larger region of small curvature, and is thus more affected by the boundary conditions.

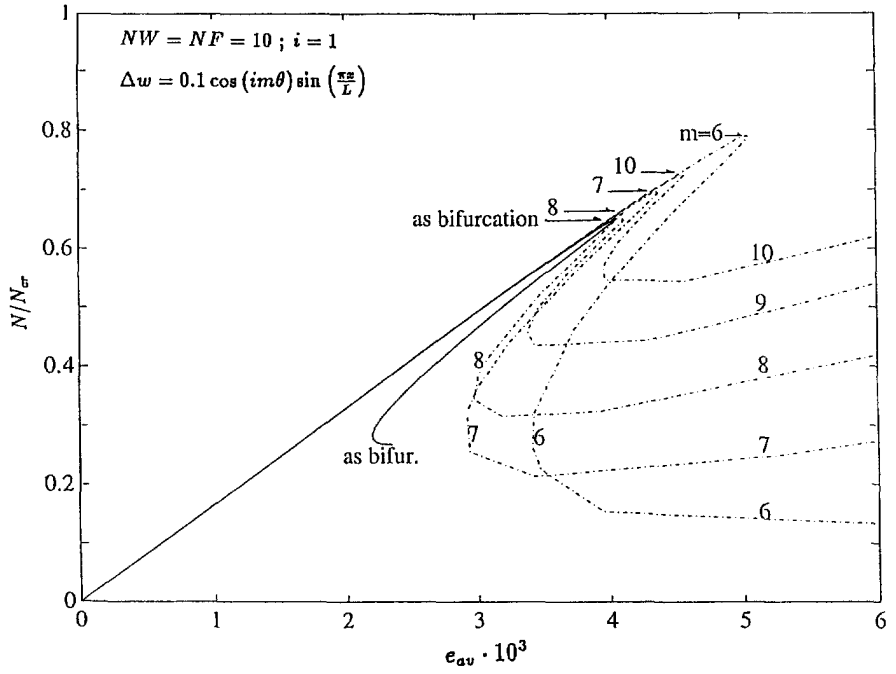


Fig. 2. Average end-shortening of circular cylindrical shells with various shapes of initial imperfections.

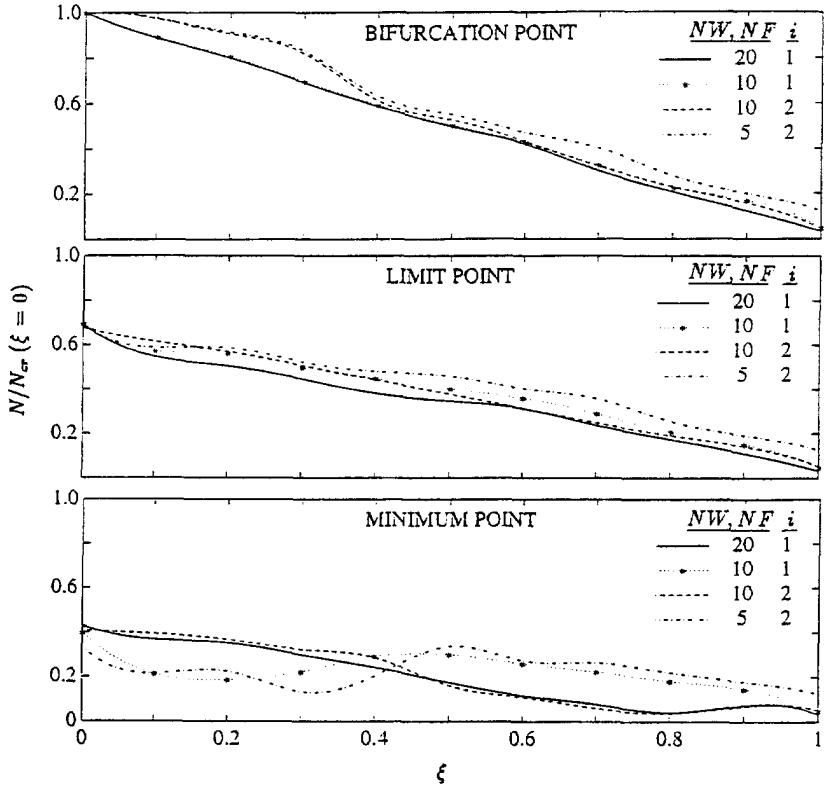


Fig. 3. Convergence with respect to the number of terms in the truncated series and characteristic wave number.

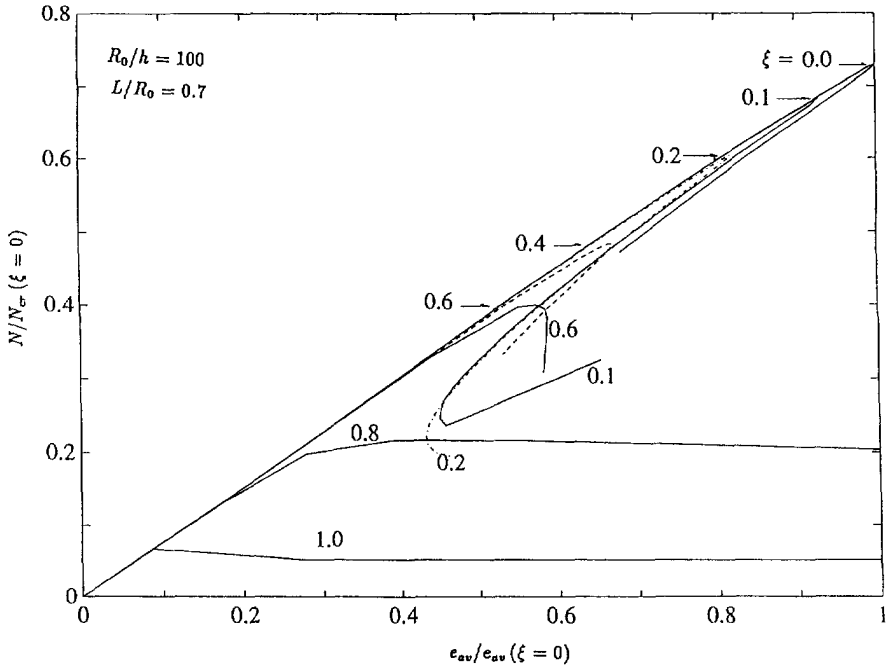


Fig. 4. Average end-shortening of oval isotropic cylindrical shells.

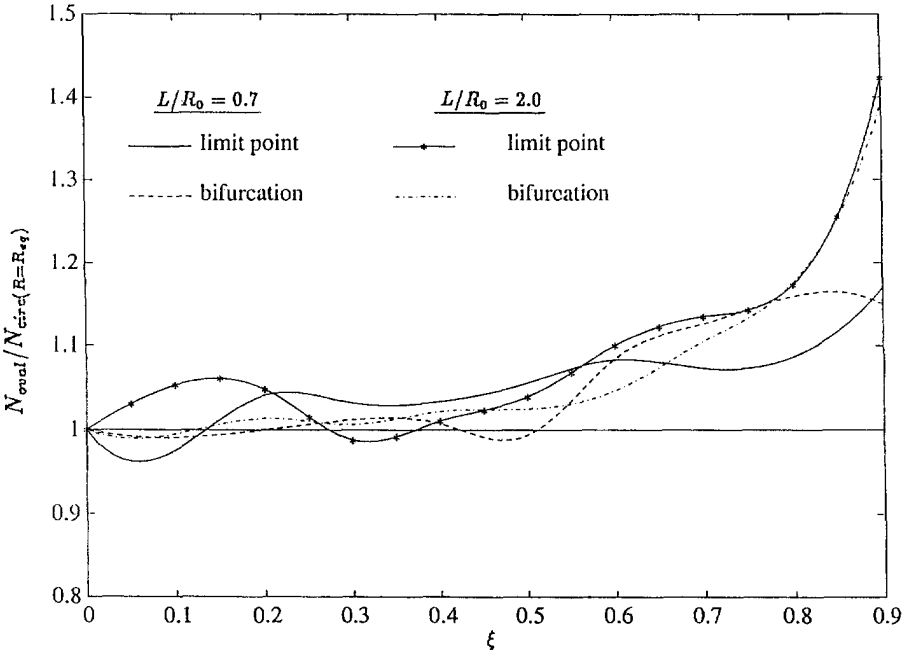


Fig. 5. Bifurcation and limit point loads versus the eccentricity of the oval cross-section.

*Laminated cylindrical shells*

The same geometric configuration considered in the isotropic examples ($R_0/h = 100$, $L/R_0 = 2.0$ and $CC_1$ boundary conditions) will now be used in the analysis of graphite/epoxy angle-ply oval cylindrical shells. Material data for the graphite/epoxy laminate are: $E_{11} = 14 \times 10^{10} \text{N/m}^2$, $E_{22} = 0.97 \times 10^{10}$ N/m$^2$, $G_{12} = 0.41 \times 10^{10}$ N/m$^2$ and $\nu_{12} = 0.26$. Ten-term expansions of the variables with the characteristic wave number $i = 1$ were used. Limit point and bifurcation loads convergence was obtained for 25 mesh points to an error of 1%. Two layer angle-ply laminates ($\pm\beta^\circ$), which behave as general orthotropic materials,

Table 1. Normalized buckling loads of isotropic oval and elliptic cylindrical shells

| Eccentricity | Oval cross-section $R_0/R(\theta) = 1+\xi\cos(2\theta)$ | | Elliptic cross-section $R_0/R(\theta) = \sum_{k=0}^{N} \alpha_k \cos(2k\theta)$ | |
|---|---|---|---|---|
| | bifurcation | limit point | bifurcation | limit point |
| Small $\xi = 0.1$ $B/A = 0.936$ $N = 1$ | 1.025 | 0.807 | 1.013 | 0.792 |
| Medium $\xi = 0.5$ $B/A = 0.711$ $N = 3$ | 0.552 | 0.444 | 0.381 | 0.321 |
| Large $\xi = 1.0$ $B/A = 0.485$ $N = 4$ | 0.056 | 0.051 | 0.078 | 0.075 |

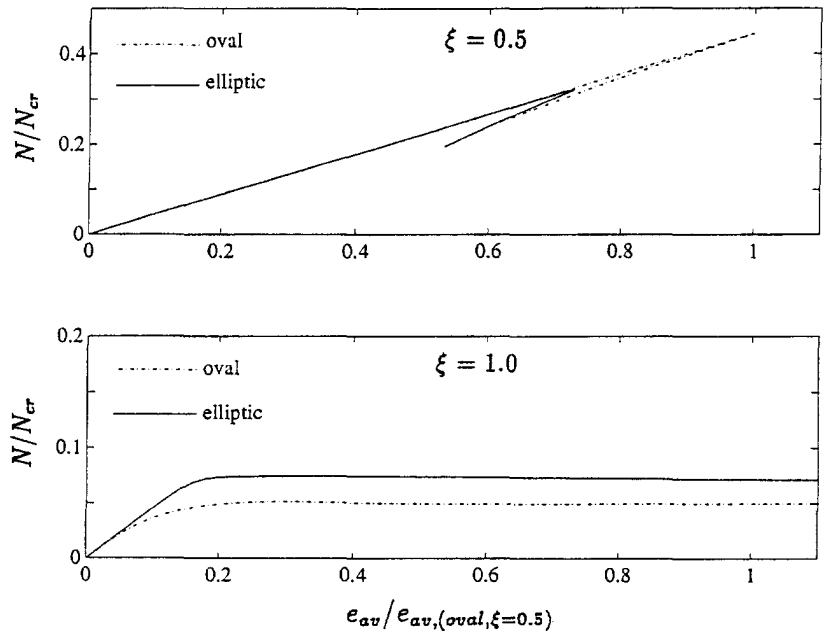


Fig. 6. Average end-shortening of oval and elliptic cylindrical shells.

were examined. Bifurcation and limit point loads versus the fiber orientation angle $\beta$ are plotted in Fig. 7. Behaviour trends for the limit point load are basically the same as observed in the linear bifurcation analysis. The large eccentricity oval cross-section, being imperfection insensitive, shows limit points almost equal to the bifurcation loads for the whole range of angle-ply laminates. The effect of the fiber orientation in small and medium eccentricity ovals is seen in Fig. 8. Even though limit point loads increase as $\beta$ increases, the pre-buckling stiffnesses decrease, up to $\beta = 60°$. For $60° \leqslant \beta \leqslant 90°$, no significant change in the pre-buckling stiffness is observed, in spite of the fact that limit points are significantly affected by changes in the fiber orientation.

## CONCLUSION

A nonlinear model and solution procedure for the analysis of non-circular cylindrical shells is presented. The non-circular cross-section is represented by expansion of the curvature into a trigonometric series, allowing for proper representation of arbitrary closed non-circular geometries. The model is able to properly handle the changes in buckling waves observed in the post-buckling behaviour of circular cylindrical shells. Imperfections in the shape of the bifurcation buckling mode seem to be of major effect in both the buckling and post-buckling stages. Unlike circular cylindrical shells, the behaviour of non-circular shells is not governed by a characteristic buckling wave and strong coupling between circumferential waves is observed. In the analysis of non-circular cylindrical shells, the

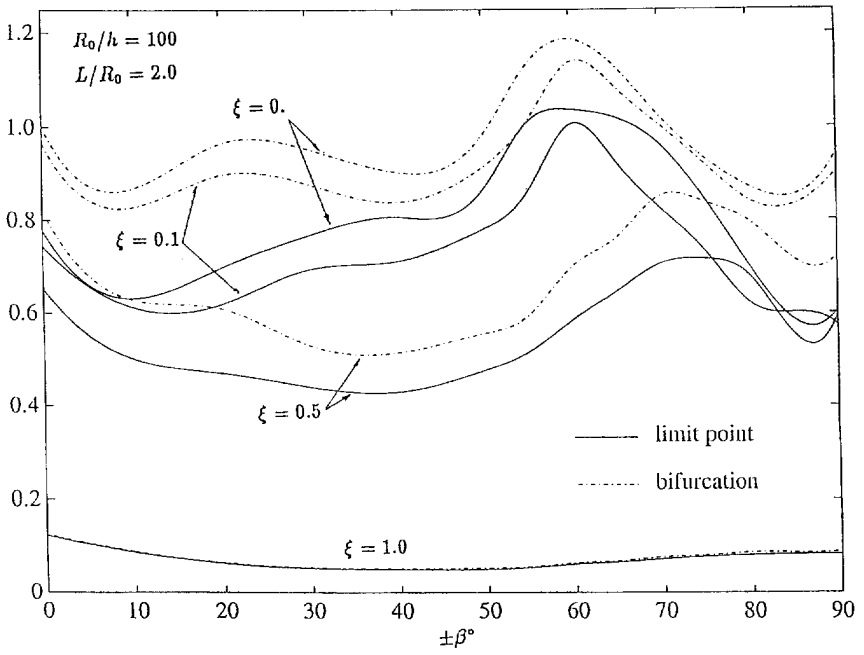


Fig. 7. Bifurcation and limit point loads versus the fiber orientation of angle-ply laminated oval shells.

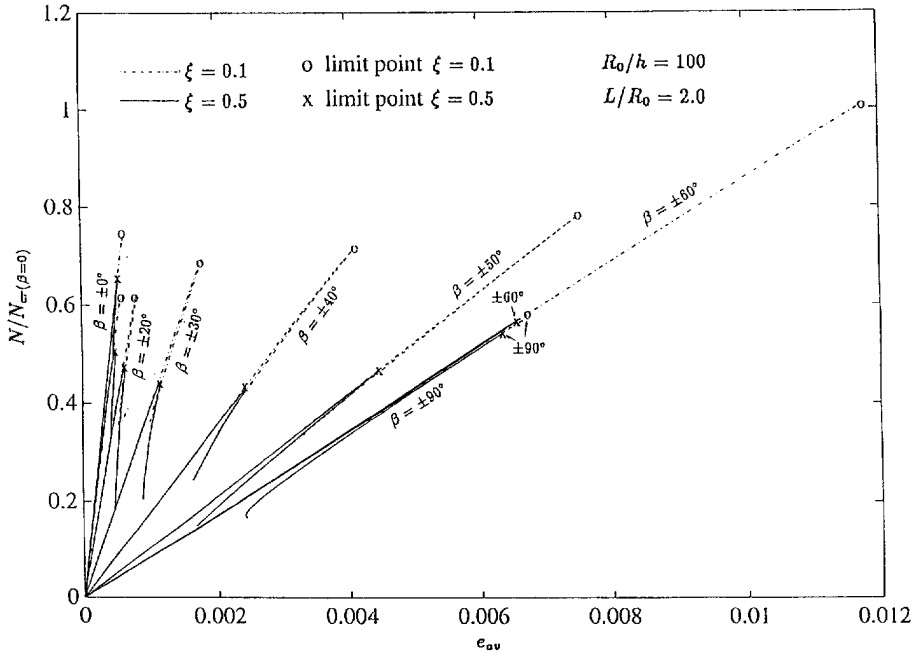


Fig. 8. Average end-shortening of angle-ply laminated oval shells.

eccentricity of the oval cross-section is shown to be a parameter of major importance on both the limit point load and the imperfection sensitivity. The largely eccentric configurations are found to be imperfection insensitive. From the analysis of angle-ply laminated oval shells we may conclude that both the bifurcation and the nonlinear behaviour are significantly affected by the laminate configuration. Finally, the simplified analytical model based on the equivalent circular cylinder is found to be too conservative and not representative.

## REFERENCES


Arbocz, J. (1974). The effects of initial imperfections on shell stability. In *Thin Shell Structures—Theory, Experiment and Design* (Edited by Y. C. Fung and E. E. Sechler), pp. 205–245. Prentice-Hall, Englewood Cliffs, N.J.

Chen, Y. N. and Kempner, J. (1976). Buckling of oval cylindrical shells under compression and asymmetric bending. *AIAA J.* **14**(9), 1235–1240.

Feinstein, G., Chen, Y. N. and Kempner, J. (1971a). Buckling of clamped oval cylindrical shells under axial loads. *AIAA J.* **9**(9), 1733–1738.

Feinstein, G., Erickson, B. and Kempner, J. (1971b). Stability of oval cylindrical shells. *J. Expl Mech.* **11**(11), 514–520.

Firer, M. (1993). Dynamic stability of laminated non-circular cylindrical shells. Ph.D. Thesis, Faculty of Civil Engineering, Technion–Israel Institute of Technology.

Hutchinson, J. W. (1968). Buckling and initial postbuckling behaviour of oval cylindrical shells under axial compression. *J. Appl. Mech. (Trans. ASME)* **35**(1), 66–72.

Kempner, J. and Chen, Y. N. (1964). Large deflections of an axially compressed oval cylindrical shell. *Eleventh Int. Congress Appl. Mech.*, pp. 299–306. Springer-Verlag, Berlin.

Kempner, J. and Chen, Y. N. (1967). Buckling and postbuckling of an axially compressed oval cylindrical shell. *Symp. on the Theory of Shells to Honor Lloyd H. Donnell*, pp. 141–183. McCuthan Pub. Co.

Narasimham, K. Y. and N. J. Hoff (1967). Calculations of the load carrying capacity of initially slightly imperfect thin-walled circular cylindrical shells of finite length. SUDAER No. 329, Department of Aeronautics and Astronautics, Stanford University.

Riks, E. (1979). An incremental approach to the solution of snapping and buckling problems. *Int. J. Solids Structures* **15**(7), 529–551.

Sheinman, I. and Firer, M. (1994). Buckling analysis of laminated cylindrical shells with arbitrary non-circular cross-section. *AIAA J.* **32**(5), 648–654.

Sheinman, I. and Simitses, G. J. (1977). Buckling analysis of geometrically imperfect stiffened cylinders under axial compression. *AIAA J.* **15**(3), 374–382.

Sheinman, I. and Simitses, G. J. (1983). Buckling and postbuckling of imperfect cylindrical shells under axial compression. *Computers Struct.* **17**(2), 277–285.

Sheinman, I., Frostig, Y. and Segal, A. (1988). Bifurcation buckling analysis of stiffened laminated composite panels. In *Buckling of Structures* (Edited by J. Arbocz, C. D. Babcook, Jr and A. Libai), pp. 355–380. Elsevier Science, Amsterdam, The Netherlands.

Simitses, G. J. (1986). Buckling and postbuckling of imperfect cylindrical shells: a review. *Appl. Mech. Rev.* **39**(10), 1517–1524.

Soldatos, K. P. and Tzivanidis, G. J. (1982). Buckling and vibration of cross-ply laminated non-circular cylindrical shells. *J. Sound Vibr.* **82**(32), 425–434.

Sun, G. (1991). Buckling and initial post-buckling behaviour of laminated oval cylindrical shells under axial compression. *J. Appl. Mech. (Trans. ASME)* **58,** 848–851.

Volpe, V., Chen, Y. N. and Kempner, J. (1978). Buckling of orthogonally stiffened finite oval cylindrical shells under axial compression and lateral pressure. POLY-M/AE 78–10, Department of Mechanical and Aerospace Engineering, Polytechnic Institute of New York.

Volpe, V., Chen, Y. N. and Kempner, J. (1980). Buckling of orthogonally stiffened finite oval cylindrical shells under axial compression. *AIAA J.* **18**(5), 571–580.